

reports of dinosterane occurrences in Proterozoic sediments from Bitter Springs and Peratataka formations, central Australia (16), and the Nonesuch Formation in the North American mid-continent rift (21). The presence of dinoflagellate relatives among acritarchs explains the continuous record of dinosteroids from Precambrian to Cenozoic source rocks from numerous localities worldwide (16, 22).

The fossilized matter available for paleontological investigation represents less than 1% of organisms that once existed on Earth. A high abundance of related specimens in a particular age suggests that there was an earlier radiation. Various kinds of simply structured, rounded acritarchs and dinoflagellate biomarkers coexist in upper Riphean rocks, although the dinoflagellate affinity of any particular Proterozoic genus requires further investigation. Dinosterane-containing acanthomorphic acritarchs are widespread in Lower Cambrian sediments. These results suggest the evolutionary sequence in which dinoflagellate ancestry originated by the Late Riphean (~800 million years ago); specimens with processes became abundant in the Early Cambrian; and finally, the branch of dinoflagellates with classical archeopyles and paratabulation developed in the Middle Triassic.

References and Notes

1. B. Dale in *Palynology: Principles and Applications*, J. Jansonius and D. C. McGregor, Eds. (American Association of Stratigraphic Palynologists Foundation, Dallas, TX, 1996), vol. 3, pp. 1249–1277.
2. D. K. Goodman, in *The Biology of Dinoflagellates*, vol. 21 of *Botanical Monographs*, F. J. R. Taylor, Ed. (Scientific Publications, Oxford, 1987), pp. 649–722; R. Helby, R. Morgan, A. D. Partridge, in *Assoc. Australas. Palaeontol. Mem.* 4 (1987), p. 1.
3. A. H. Knoll, in (1), vol. 1, pp. 51–81.
4. J. H. Lipps, in *Fossil Prokaryotes and Protists*, J. H. Lipps, Ed. (Blackwell, Boston, 1993), pp. 1–10.
5. L. Margulis and K. V. Schwartz, *Five Kingdoms: An Illustrated Guide to the Phyla of Life* (Freeman, San Francisco, 1982).
6. H. Tappan, *The Paleobiology of Plant Protists* (Freeman, San Francisco, 1980); C. V. Mendelson, in (4), pp. 77–104.
7. D. M. Anderson, J. J. Lively, E. M. Reardon, C. A. Price, *Limnol. Oceanogr.* 30, 1000 (1985).
8. F. Martin and G. Kjellström, *Neusser Jahrb. Geol. Palaeontol. Monatsh.* 1973, 44 (1973).
9. D. Wall and B. Dale, *Micropaleontology* 14, 265 (1968).
10. R. A. Fensome et al., *Micropaleontol. Spec. Pap.* 7 (1993).
11. K. Mens, J. Bergström, K. Lendzion, *Valgus Tallin.* 1987 14 (1987).
12. D. Guy-Ohlson and G. T. Boalch, *Phycologia* 31, 523 (1992).
13. J. M. Hayes, I. R. Kaplan, K. M. Wedeking, in *Earth's Earliest Biosphere. Its Origin and Evolution*, J. W. Schopf, Ed. (Princeton Univ. Press, Princeton, NJ, 1983), pp. 93–134.
14. N. M. Talyzina, *Rev. Palaeobot. Palynol.* 100, 99 (1998).
15. G. A. Warburton and J. E. Zumberge, *Anal. Chem.* 55, 123 (1983).
16. R. E. Summons and M. R. Walter, *Am. J. Sci.* 290-A, 212 (1990).
17. J. K. Volkman, S. M. Barrett, G. A. Dunstan, S. W. Jeffrey, *Org. Geochem.* 20, 7 (1993).
18. N. Withers, in *The Biology of Dinoflagellates*, vol. 21 of *Botanical Monographs*, F. J. R. Taylor, Ed. (Scientific Publications, Oxford, 1987), pp. 316–359.
19. J. K. Volkman, P. Kearney, S. W. Jeffrey, *Org. Geochem.* 15, 489 (1990).
20. K. E. Peters and J. M. Moldowan, *The Biomarker Guide. Interpreting Molecular Fossils in Petroleum and Ancient Sediments* (Prentice-Hall, Englewood Cliffs, NJ, 1993).
21. L. M. Pratt, R. E. Summons, G. B. Hieshima, *Geochim. Cosmochim. Acta* 55, 911 (1991).
22. J. M. Moldowan et al., *Geology* 24, 159 (1996); J. M. Moldowan et al., in *Ecology of the Cambrian Radiation*, A. Zhuravlev and R. Riding, Eds. (Cambridge Univ. Press, Cambridge, in press).
23. This work, supported by a postgraduate fellowship, a Swedish Natural Science Research Council (NFR) grant to G. Vidal, and a NASA Planetary Biology Internship, forms part of the doctoral thesis project of N.T., which began under the supervision of the late G. Vidal. A. Johannisson provided expertise on the FACS instrument. Chemical analytical work was assisted by F. J. Fago and supported by donations to the Stanford University Molecular Organic Geochemistry Industrial Affiliates program. Reviews by P. H. Ostrom, P. Albrecht, J. Peel, and M. Moczydlowska improved the report.

28 April 1998; accepted 10 July 1998

Moho Offset Across the Northern Margin of the Tibetan Plateau

Lupei Zhu* and Donald V. Helmberger

Anomalous double-pulse teleseismic *P*-wave arrivals were observed at one station near the northern margin of the Tibetan Plateau. The azimuthal dependence of the waveform distortion and its absence at nearby stations indicated that the distortion was produced by receiver-side crustal heterogeneity. Modeling of the three-component data revealed a 15- to 20-kilometer Moho offset that occurs over a narrow lateral range of less than 5 kilometers. This east-west-striking offset separates the thick Tibetan Plateau crust from the Qaidam Basin crust. Such a sharp crustal thickness change implies a weak Tibetan Plateau crust that thickens vertically in response to penetration by India from the south and to blockage caused by a strong Qaidam Basin crust to the north.

The uplift of the Tibetan Plateau is the result of thickened crust arising from the India-Eurasia collision and the subsequent penetration of India into Eurasia. However, the mechanisms of crustal thickening are debated (1). Lateral heterogeneities of crustal strength are believed to play a role in determining the magnitude and distribution of deformation in a continent-continent collision (2, 3). The plateau has a fairly uniform elevation of about 5 km, surrounded by several low-lying sedimentary basins: the Tarim Basin to the northwest, the Qaidam Basin to the north, and the Sichuan Basin to the east (Fig. 1A). These basins are underlain by stable Precambrian cratons, which have experienced little deformation since the Paleozoic (1, 4). The transition of lithospheric structure from the plateau to these cratons is poorly constrained. From the analysis of teleseismic *P* waveforms, we present a model of a relatively sharp step in the Moho across the northern margin of the Tibetan Plateau.

During the 1991–1992 Sino–U.S. Tibet

seismic experiment, 11 broadband stations were deployed along the Golmud-Lhasa highway (5) (Fig. 1A). One of the stations, TUNL, was located in the foothills of the Kunlun mountain range, which runs east and west and marks the northern boundary of the Tibetan Plateau (Fig. 1B). About 300 teleseismic events (distance range >30°) were recorded with good signal-to-noise ratios. For each event, we aligned the records of all the stations with the onsets of the *P* wave to examine the waveform variation across the array. Generally, the vertical component of the teleseismic *P* wave is less sensitive to structure near the recording site because of the wave's nearly vertical incident ray path. For this reason, the vertical component is often treated as an effective source time function of the earthquake in receiver function analyses (6). However, if crustal heterogeneity exists, then waveform distortion can occur. The *P* waveforms at TUNL consistently showed double-pulse arrivals from events in directions from N45°E to N70°E (Fig. 2A). Although the amplitudes of the *P* waves varied from station to station, the waveforms at most stations had a similar single-pulse shape, which is expected for the epicentral distances from a moderate earthquake at depths >40 km. However, the waveforms at TUNL consisted of two pulses separated by ~1 s. Because the similarity of waveforms at other stations ruled out the pos-

Seismological Laboratory, California Institute of Technology, Pasadena, CA 91125, USA.

*To whom correspondence should be addressed. E-mail: lupei@usc.edu. Present address: Southern California Earthquake Center, University of Southern California, Los Angeles, CA 90089, USA.

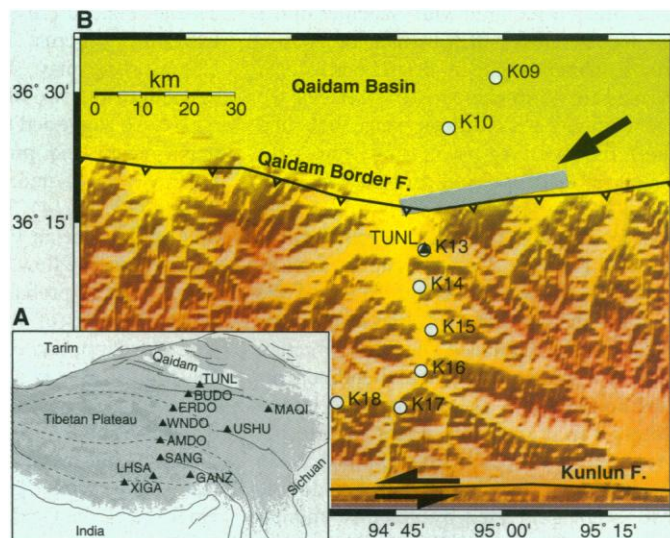
REPORTS

sibility of a complex event source time function, we concluded that the double pulses were caused by the multipathing of wave propagation through a laterally varying velocity structure on the receiver side. Both pulses had the same polarity on the vertical component, which indicated that they were direct P -wave arrivals. Any surface reflection near the station could generate a delayed P -wave pulse, provided that a shallow structure (for example, the bottom of a sediment wedge) reflected it back to the station, but the polarity would be reversed by the free-surface reflection. In addition, multiple P -wave reflections within the crust reduce the amplitude of the subsequent pulses because of the nearly vertical incidence angle.

We estimated the depth z of the anomalous structure by examining the size of the Fresnel zone R at the surface. From the classical theory of optics, $R = \sqrt{\lambda z}$, where λ is the wavelength, which is about 10 km for teleseismic P waves, and R is equivalent to the surface area where the double-pulse waveform can be observed. Unfortunately, the station spacing of the experiment is >100 km, so we cannot constrain R . In 1993, another seismic experiment was conducted by Chinese and French scientists, in which 50 stations were deployed along a north-south profile from the Qaidam Basin to central Tibet (7). The experiment was operated for 3 months and used mostly short-period instruments. Station K13 in this experiment was located at the same site as TUNL. The same double-pulse waveforms were observed at K13 for events from the same azimuth range as the TUNL events (Fig. 2B). However, the nearby stations (K10, K14, K15, and K17) did not show this distortion. The lack of distortion helped us to constrain R to be <25 km (half of the distance between K10 and K14), which produced a depth estimate of <60 km for the velocity anomaly.

Also, TUNL was the station in the broadband array with the strongest azimuthal variation of teleseismic arrival times; the first P -wave arrivals coming from the northern azimuth were ~ 1 s faster than those coming from the south (Fig. 3). This variation indicates that the average P -wave velocity of the crust and upper mantle is faster under the Qaidam Basin than under the Tibetan Plateau. The double pulse occurs in the narrow azimuth window of the transition from faster to slower arrivals, where the wave field samples two distinct velocities (Fig. 3). If we assume that the velocity anomaly is in the crust and that the crustal P -wave velocity of the Tibetan Plateau is 6.1 to 6.3 km/s (8, 9), then a separation of the two pulses by 1 s through a 50-km-thick crust requires an average P -wave velocity of 6.8 to 7.0 km/s for the Qaidam Basin crust. The velocity of the lower crust could be higher if the thick low-velocity sedimentary layer of the basin is

Fig. 1. (A) Map of the Tibetan Plateau and surrounding areas. Light and dark shading indicate elevation above 3 and 5 km, respectively. Solid lines indicate major faults, and dashed lines indicate sutures. Solid triangles represent broadband stations of the 1991–1992 Sino–U.S. Tibet seismic experiment. (B) The northern Tibetan margin near broadband station TUNL (solid triangle), where anomalous double-pulse P waveforms were observed for events from the east-northeast direction (indicated by the arrow). Open circles represent short-period stations of the 1993 Sino–French Lithoscope Kunlun experiment. The location of the Moho offset is shown by the gray bar.



considered. Such high velocity values are not realistic for crustal material. Therefore, the structure that could explain the double pulse would have a thinner crust under the Qaidam Basin so that the velocity contrast between the lower crust of the Tibetan Plateau and the uppermost mantle of the Qaidam Basin would provide the desired lateral velocity variation.

We used the Kirchhoff-Helmholtz integral (10) to calculate the wave propagation through a three-dimensional (3D) Moho. Our model setup and the location of the receiver (TUNL) are illustrated in Fig. 4; however, the whole crust was simplified to a layer with a P -wave velocity of 6.3 km/s in the calcula-

tion. We used forward modeling to determine the location, orientation, height, and width of the Moho offset. Our calculation indicates that the occurrence of the second pulse and its relative amplitude are sensitive to the azimuths of incoming rays and to the width of the offset (Figs. 3 and 5A). This dependence leads to constraints on the strike ($N80^\circ E$) and on the width (<5 km) of the offset. The height of the offset is determined by the separation of the two pulses and thus trades off with the velocity contrast between the lower crust of the Tibetan Plateau and the uppermost mantle of the Qaidam Basin. A

Fig. 2. (A) Vertical components of broadband velocity records from a magnitude 5.5 earthquake that occurred 49 km beneath the Kuril Islands (13 December 1991, 0800 UTC). Relative amplitudes are plotted. Station names appear at the right; the numbers under the station names are epicentral distances in degrees. Arrows point to the anomalous double-pulse P waveform shape at stations TUNL (A) and K13 (B). (B) Vertical components of short-period velocity records from an event in the same source region (normalized amplitudes are plotted because the station gain factors are not available).

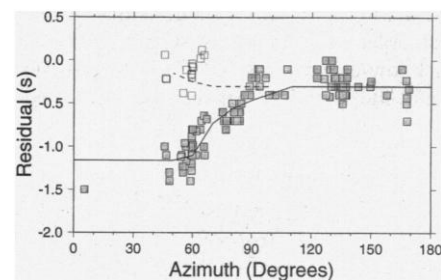
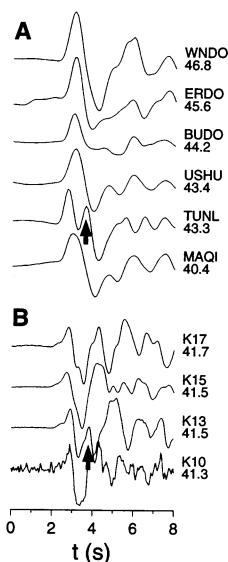


Fig. 3. Travel-time residuals of the first P -wave arrivals (shaded squares) at station TUNL from earthquakes in a distance range of 30° to 50° . Positive values are early arrivals with respect to the theoretical travel times of the IASPEI91 Earth model by the International Association of Seismology and Physics of the Earth's Interior (17). For each event, the residual at station BU DO was subtracted to remove the uncertainty of event origin time and source region heterogeneity; BU DO was chosen because it was the closest reference station to TUNL and it showed little azimuthal variation of teleseismic arrival time (18). Open squares represent the second pulses of the anomalous P waveforms. Solid and dashed lines indicate the predicted arrival times of the first and second pulses by the Moho offset model, respectively.

REPORTS

20-km offset is required with velocities of 6.3 km/s for the crust and 8.1 km/s for the uppermost mantle in our model. The predicted *P* waveform from the Moho offset fits the three components (vertical, tangential, and radial) of observed waveforms (Fig. 5B). This correspondence confirms that the wave field is *P*-wave energy, arriving askew with respect to the great circle (as indicated by the tangential motion). Also, a complex shallow structure is eliminated as the cause of the waveform distortion because the *P*-to-*S* converted waves produced by the structure would be apparent on the radial component.

Although there is evidence of lateral velocity variation in the upper mantle between northern Tibet and the Qaidam Basin (11), our analysis shows that the double pulse is not generated by velocity anomalies below 60 km. Mantle velocity anomalies are usually associated with temperature variation; therefore, they may not be sharp enough to cause multipathing to relatively short-wavelength body waves. The crustal velocity difference between the Tibetan Plateau and the Qaidam Basin, however, could contribute to the separation of the two pulses, but the amount is limited. If we increase the *P*-wave velocity of the Qaidam lower crust to 6.7 km/s, a 15-km Moho offset is still required.

Our model of a sharp Moho offset across the northern margin of the Tibetan Plateau has several implications for crustal deformation and plateau evolution. (i) The offset is located directly beneath the northern margin of the Tibetan Plateau, where the surface elevation increases abruptly from 3 to 5 km (Fig. 4). The correlation between the surface and Moho topographies suggests that, to the first order, the plateau is supported by its thick low-density crust. (ii) The Moho offset marks the boundary between the thickened

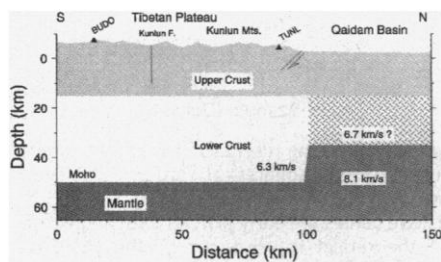


Fig. 4. A north-south cross section along the 95°E meridian showing the surface topography (exaggerated by a factor of 2), major faults, and the possible crustal structure used in modeling *P* waveforms at TUNL. Previous studies showed that the crustal thickness of northern Tibet is about 55 km (8, 13, 18). The division of the crust into upper and lower parts at a depth of 20 km (relative to the surface) is approximate, but there is ample evidence that indicates the existence of a low-velocity lower crust in northern Tibet (8, 13, 14).

Tibetan Plateau crust and the less deformed Qaidam Basin crust. The difference in deformation style may stem from the relative strength of the two blocks. Seismic observations have suggested the existence of a “hot” upper mantle and, probably, a partially molten lower crust under central and northern Tibet (8, 9, 12–14). Therefore, the deformation of the Tibetan Plateau lower crust may occur by ductile flow. In contrast, the Qaidam Basin crust is probably brittle down to the Moho because of its crustal composition, cold geotherm, and old age (2). The Qaidam Basin crust acts as a rigid block that resists the northward lower crustal flow of the Tibetan Plateau, which is induced by the penetration of India. As a result, the Tibetan Plateau lower crust grows vertically. Such blockage by the Qaidam Basin crust and other surrounding cratons confines the deformation of the Tibetan Plateau crust to a limited volume and raises the plateau uniformly (15, 16). (iii) The lack of a direct connection between the Kunlun fault and the Moho offset suggests that the fault is limited to the brittle upper crust. The Kunlun fault and the Altyn Tagh fault, two large east-west-oriented strike-slip faults, are often thought to bound the Tibetan Plateau from the neighboring cratons, despite being located 50 to 100 km inside the plateau. These faults might be initiated or reactivated by the lower crustal flow as the material moves to the east and south, where a leakage exists (16).

The existence of an abrupt change of

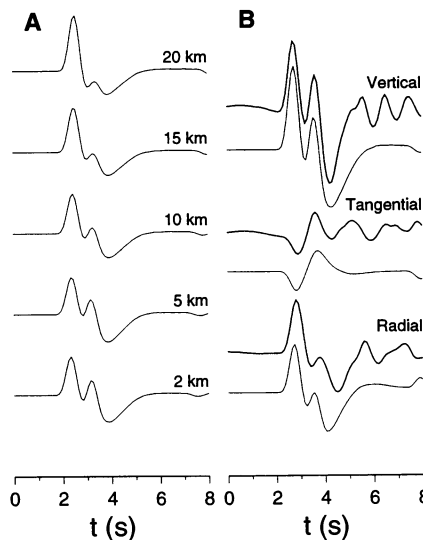


Fig. 5. (A) Sensitivity of the *P* waveform to the width of the Moho offset, where the height of the offset is 20 km and the incoming teleseismic ray is from N60°E. The amplitude of the second pulse decreases substantially as the offset becomes wider than 5 km. (B) Comparison of the observed three-component *P* waveforms with the waveforms predicted by our best Moho offset model (strike, N80°E; width, 2 km; height, 20 km).

Moho topography also raises concern about 3D seismic tomography studies, which usually assume a flat Moho in their starting model and invert travel-time residuals for velocity perturbations in the crust and mantle (7). Our modeling shows that about 90% of the travel-time residuals are produced by the Moho offset (Fig. 3), and if ignored, this offset would be mapped into the upper mantle velocity variation because of the embedded poor vertical resolution in teleseismic travel-time inversions. Whereas the double-pulse waveforms at station TUNL represent a rare case of distortion by abrupt structural variation, smoothly varying Moho topography will modulate waveforms in a more subtle way, either sharpening or broadening the *P* waveform pulse, as seen at other stations (Fig. 2A). With the increasing deployments of broadband arrays in tectonically interesting regions, the use of waveform data in addition to travel-time measurements cannot be overemphasized.

References and Notes

1. J. F. Dewey, R. M. Shackleton, C. Chang, Y. Sun, *Philos. Trans. R. Soc. London Ser. A* **327**, 379 (1988).
2. P. Molnar and P. Tapponnier, *Earth Planet. Sci. Lett.* **52**, 107 (1981).
3. P. C. England and G. A. Houseman, *Nature* **315**, 297 (1985).
4. S. Maruyama, J. G. Liou, T. Seno, in *The Evolution of the Pacific Ocean Margins*, Z. Ben-Avraham, Ed. (Oxford Univ. Press, New York, 1989), pp. 75–99; A. Yin and S. Nie, in *Tectonic Evolution of Asia*, A. Yin and T. M. Harrison, Eds. (Cambridge Univ. Press, New York, 1996), pp. 442–485.
5. T. J. Owens, G. E. Randall, F. T. Wu, R. S. Zeng, *Bull. Seismol. Soc. Am.* **83**, 1959 (1993).
6. C. A. Langston, *ibid.* **67**, 1029 (1977).
7. G. Wittlinger et al., *Earth Planet. Sci. Lett.* **139**, 263 (1996).
8. T. J. Owens and G. Zandt, *Nature* **387**, 37 (1997).
9. A. J. Rodgers and S. Y. Schwartz, *J. Geophys. Res.* **103**, 7137 (1998).
10. F. J. Hilterman, *Geophysics* **40**, 745 (1975); P. Scott and D. V. Helmberger, *Geophys. J. R. Astron. Soc.* **72**, 237 (1983); F. Neele and R. Snieder, *Geophys. J. Int.* **109**, 670 (1992); S. Vanderlee, H. Paulssen, G. Nolet, *Phys. Earth Planet. Inter.* **86**, 147 (1994).
11. L. S. Zhao and J. Xie, *Geophys. J. Int.* **115**, 1070 (1993); D. E. McNamara, W. R. Walter, T. J. Owens, C. J. Ammon, *J. Geophys. Res.* **102**, 493 (1997).
12. J. Ni and M. Barazangi, *Geophys. J. R. Astron. Soc.* **72**, 665 (1983).
13. C. Brandon and B. Romanowicz, *J. Geophys. Res.* **91**, 6547 (1986).
14. L. Zhu, T. J. Owens, G. E. Randall, *Bull. Seismol. Soc. Am.* **85**, 1531 (1995).
15. W. Zhao and J. Morgan, *Tectonics* **4**, 359 (1985); *ibid.* **6**, 489 (1987).
16. R. Westaway, *J. Geophys. Res.* **100**, 15173 (1995).
17. L. N. Kennett and E. R. Engdahl, *Geophys. J. Int.* **105**, 429 (1991).
18. L. Zhu, thesis, California Institute of Technology, Pasadena (1998).
19. Comments by M. Simons, B. Keller, T. Melbourne, and two anonymous reviewers have helped to improve the manuscript. We thank G. Poupinet and A. Paul for providing the Sino-French 1993 Lithoscope Kunlun experiment data. This work has been supported by NSF grant EAR-9725808. This is Division of Geological and Planetary Sciences, California Institute of Technology contribution 8544 and Southern California Earthquake Center contribution 443.

24 March 1998; accepted 14 July 1998